

# Composition and Structure of the $\alpha$ -AlF<sub>3</sub>(0001) Surface

A. Wander,<sup>\*,†</sup> B. G. Searle,<sup>‡</sup> C. L. Bailey,<sup>§</sup> and N. M. Harrison<sup>⊥</sup>

CCLRD Daresbury Laboratory, Warrington, Cheshire, WA4 4AD, United Kingdom

Received: May 20, 2005; In Final Form: September 26, 2005

Strong Lewis acid catalysts are widely used in a variety of industrial processes including Cl/F exchange reactions. Aluminum fluorides (AlF<sub>3</sub>) have great potential for use in such reactions. Despite the importance of the surface in the catalytic process little is known about the detailed atomic scale structure of AlF<sub>3</sub> surfaces. In the current study we employ state of the art surface thermodynamics calculations based on hybrid-exchange density functional theory to predict the composition and structure of the basal plane surface of  $\alpha$ -AlF<sub>3</sub> for the first time. We examine four possible terminations of the  $\alpha$ -AlF<sub>3</sub> (0001) surface and demonstrate that the surface is terminated by a layer containing two fluorine atoms per cell at all realistic fluorine partial pressures. The fluorine ions in the outermost layer of the material reconstruct to mask the Al<sup>3+</sup> ion from the external gas phase and consequently we would expect this surface to be inactive as a Lewis acid catalyst in line with experimental observation.

## 1. Introduction

The catalytic fluorination of hydrocarbons produces a rich and diverse chemistry that is of great industrial importance. For many years these catalysts have facilitated the large-scale production of chlorofluorocarbons for a wide range of applications including aerosol propellants, refrigerants, and solvents.<sup>1,2</sup> Fluorination is now playing a growing role in inorganic synthesis as it provides a powerful tool for tuning electronic, chemical, optical, and mechanical properties. Aluminum fluorides are of great interest as potential strong Lewis acid solid catalysts. High surface area aluminum fluoride can be prepared that has a Lewis acidity comparable to that of the widely used Swarts catalysts based on antimony pentafluoride.<sup>3,4</sup> This makes it a promising candidate for use in several Lewis acid catalyzed reactions including Cl/F exchange which have been extensively studied.<sup>5–12</sup> Despite this, very little is known about the detailed surface structure of these fluorides although models have been suggested based on observations of chemical activity.<sup>11</sup>

It is known that the  $\alpha$ -AlF<sub>3</sub> surfaces are chemically inert and it appears likely that the chemically active surfaces of the high surface area AlF<sub>3</sub> material are those of the  $\beta$  phase.<sup>13</sup> An understanding of the difference in reactivity between these two phases of the material may be of fundamental importance in any future attempts to design real catalysts based on AlF<sub>3</sub>. Geometrically, the surfaces of the  $\alpha$  phase are far more simple than the  $\beta$  phase. Consequently it is logical to begin by investigating the surface structure and composition of the  $\alpha$ -phase. In the current study we have therefore examined the surface structure of  $\alpha$ -AlF<sub>3</sub> in an effort to understand why its surfaces are chemically inert.

The bulk  $\alpha$ -AlF<sub>3</sub> structure is closely related to the corundum structure adopted by  $\alpha$ -Al<sub>2</sub>O<sub>3</sub> but with one of the aluminum sites occupied in the oxide being vacant in the fluoride. The

surfaces of alumina have been widely studied and it is known that the basal plane (the (0001)) surface is very stable.<sup>14</sup> We have therefore begun our investigation of  $\alpha$ -AlF<sub>3</sub> by considering the structure of its basal plane (0001) surface.

Recently it has been demonstrated that the effects of an external atmosphere of oxygen on the surface structure of oxide materials can be included in first principles calculations<sup>15–17</sup> via the inclusion of an oxygen chemical potential that is a function of oxygen partial pressure and temperature. The inclusion of such effects allows first principles simulation to move away from their traditional point in phase space of zero temperature and pressure and begin to study materials in environments of more relevance to catalytic processes. In the current study we use this formalism to consider the structure of the  $\alpha$ -AlF<sub>3</sub> surface as a function of fluorine chemical potential.

## 2. Methodology

The relative stability of a surface with variable stoichiometry is determined by minimization of the surface free energy. A mechanism for computing the surface free energy from ab initio calculations has been developed<sup>15,16</sup> and has been described recently by Reuter and Scheffler.<sup>17</sup> Here, a brief outline of the formalism as applied in this article is presented. Modeling the fluoride surface as a slab of material periodic in two dimensions and of finite thickness in the third, the surface free energy may be defined as<sup>18</sup>

$$\gamma(T,P)A = G_{\text{slab}}(T,P) - N_{\text{M}}\mu_{\text{M}}(T,P) - N_{\text{F}}\mu_{\text{F}}(T,P) \quad (1)$$

in which  $A$  is the surface area of the unit cell (counting both surfaces of the slab),  $G_{\text{slab}}$  is the Gibbs energy per unit cell of the slab, and  $N_{\text{M}}$  and  $N_{\text{F}}$  are respectively the total number of metal and fluorine ions within the slab.  $\mu_{\text{M}}$  and  $\mu_{\text{F}}$  are the chemical potentials per atom of the pure metal and the fluorine gas, respectively.

As the surface is in equilibrium with the bulk fluoride  $\mu_{\text{M}}$  and  $\mu_{\text{F}}$  cannot vary freely as they are constrained to satisfy

$$g_{\text{bulk}} = m\mu_{\text{M}} + n\mu_{\text{F}} \quad (2)$$

\* Address correspondence to this author.

† E-mail: a.wander@dl.ac.uk.

‡ E-mail: b.g.searle@dl.ac.uk.

§ E-mail: c.l.bailey@dl.ac.uk.

⊥ E-mail: n.m.harrison@dl.ac.uk.

where the fluoride has the stoichiometry  $M_mF_n$  and  $g_{\text{bulk}}$  is the Gibbs free energy per formula unit of the bulk crystal. Here, the variation of surface stoichiometry with  $\mu_F$  is of interest so this constraint is used to eliminate  $\mu_M$  from eq 1. Defining the surface fluorine excess as

$$\Gamma_F = \left( N_F - \frac{nN_M}{m} \right) \quad (3)$$

one may write the surface free energy as

$$\gamma(T, P) = \frac{1}{A} \left( G_{\text{slab}}(T, P) - \frac{1}{m} N_M g_{\text{bulk}} - \Gamma_F \mu_F(T, P) \right) \quad (4)$$

In practice the fluorine chemical potential is controlled by varying the fluorine partial pressure and temperature. Approximating fluorine as an ideal gas, the chemical potential is given by

$$\mu_F(T, P) = \mu_F(T, P^0) + \frac{1}{2} kT \ln \left( \frac{P}{P^0} \right) \quad (5)$$

Thus the complete temperature and pressure dependence of the fluorine chemical potential is determined relative to its value at a reference pressure  $P^0$ . The chemical potential must be defined with respect to an energy zero, which is consistent with that used to compute the bulk and slab free energies defined in eq 4. For the ideal gas a suitable reference energy is the athermal limit at which the chemical potential equals the energy of formation of a single molecule for any pressure; thus the reference energy for  $\mu_F(T, P)$  is taken to be

$$\mu_F(0, P) = \frac{1}{2} E_{F_2}^{\text{total}} \equiv 0 \quad (6)$$

The chemical potential at a reference pressure may then be obtained from the measured variation of the free energy as

$$\mu_F(T, P^0) = \mu_F(0, P^0) + \frac{1}{2} \Delta G(\Delta T, P^0, F_2) = \frac{1}{2} [H(T, P^0, F_2) - H(0K, P^0, F_2)] - \frac{1}{2} T [S(T, P^0, F_2) - S(0K, P^0, F_2)] \quad (7)$$

The enthalpy and entropy of gaseous fluorine at standard pressure are tabulated in thermochemical data tables<sup>19</sup> and may be extrapolated to the athermal limit.

In practice the Gibb's free energies of the slab and bulk crystal are computed at the athermal limit and their temperature dependence is ignored as it is negligible compared to that of the gas. Correction to finite temperature is possible by either molecular dynamics simulation or the calculation of the lattice dynamics and the use of the quasiharmonic approximation. However, as the current article is concerned with the qualitative behavior of the surface stability rather than a quantitative determination of the absolute surface formation energy these small corrections have not been computed. The small PV term due to the change in volume of the surface and bulk phases is also neglected. This approximation is in line with previous first principles studies of the surface free energy.<sup>15–17</sup>

Calculations were performed with the CRYSTAL code<sup>20</sup> and the B3LYP hybrid exchange functional, which has been shown to provide reliable structures and energetics in a wide range of materials.<sup>21</sup> The bulk unit cell of  $\alpha\text{-AlF}_3$  is defined by four parameters: the  $a$  and  $c$  lattice vectors of the unit cell and the fractional coordinates of the  $F^-$  ions. The  $\text{Al}^{3+}$  ions are located at the positions (0.0, 0.0, 0.0) and (0.0, 0.0, 0.5) while the F

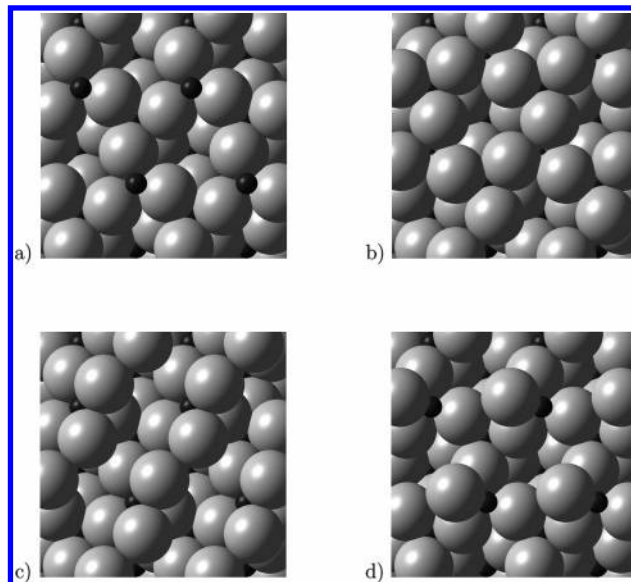


**Figure 1.** Possible terminations of the  $\alpha\text{-AlF}_3$  (0001) surface: (a) the aluminum terminated  $S_{\text{Al}}$  slab, (b) the  $S_{3\text{F}}$  slab, (c) the  $S_{2\text{F}}$  slab, and (d) the  $S_{1\text{F}}$  slab.

**TABLE 1: Summary of Bulk  $\alpha\text{-AlF}_3$  Structures**

study	$a$ (Å)	$c$ (Å)	$x$ (fractional)	$y$ (fractional)
this study	5.009	12.631	0.0996	0.0835
experiment <sup>23</sup>	4.925	12.448	0.0922	0.0830

ion is located at position  $(x, 0.3333, y)$ . We began our investigation by performing a full structure optimization of the bulk geometry of  $\alpha\text{-AlF}_3$ . Optimization of bulk and surface structures was performed by energy minimization, using an unconstrained Broyden–Fletcher–Goldfarb–Shanno (BFGS) algorithm as implemented in the DOMIN software.<sup>22</sup> The atomic positions were allowed to relax in all directions consistent with the symmetry. For cell optimization the stresses were calculated by numerical differentiation with a finite difference step of 0.002 Å, while for optimization of atomic positions analytic derivatives of the energy were employed.

The results of the lattice optimization are shown in Table 1. The calculated equilibrium lattice constants for the hexagonal unit cell and the nonsymmetry fixed positions of the atoms agree with those observed to within 2%.

The relative charges on the atoms were calculated by using a Mulliken partition of the total charge density. This is a somewhat arbitrary choice, since there is no unique method of performing the partition of the charge density. However, the choice of a given scheme is still extremely useful in comparing the results of calculations performed with use of similar basis sets.<sup>24</sup> It therefore provides a useful tool for comparing charge distributions of bulk and surface calculations, and for examining the effects of differing treatments of electronic exchange and correlation.

### 3. Results and Discussion

Several terminations of  $\alpha\text{-AlF}_3$  are possible and are displayed in Figure 1. The crystal structure consists of planes containing 3  $F^-$  ions and planes containing a single  $\text{Al}^{3+}$  ion stacked along the  $c$  axis. Consequently two terminations of the crystal are achieved simply by termination on each such plane. In addition we have considered two further terminations created by successive removal of  $F^-$  ions from the fluorine terminated surface.

For these surface calculations a periodic two-dimensional slab of material was used. The boundary condition perpendicular to

**TABLE 2: The Structure of the S<sub>Al</sub> Slab<sup>a</sup>**

atom	$\Delta x$	$\Delta y$	$\Delta z$
Al <sub>1</sub>	—	—	−0.134
F <sub>2</sub>	0.028	−0.246	0.046
Al <sub>3</sub>	—	—	−0.008
F <sub>4</sub>	−0.029	0.061	−0.007
Al <sub>5</sub>	—	—	−0.001
F <sub>6</sub>	0.009	−0.010	−0.003

<sup>a</sup> Values quoted are displacements of ions away from the bulk terminated positions in Å. Displacements constrained by symmetry to be zero are indicated by —. The subscripts on the atom types refer to the layer number of the atom.

**TABLE 3: The Structure of the S<sub>3F</sub> Slab<sup>a</sup>**

atom	$\Delta x$	$\Delta y$	$\Delta z$
F <sub>1</sub>	0.063	−0.211	0.113
Al <sub>2</sub>	—	—	−0.011
F <sub>3</sub>	−0.031	0.061	0.003
Al <sub>4</sub>	—	—	0.000
F <sub>5</sub>	0.018	−0.026	0.002
Al <sub>6</sub>	—	—	−0.008
F <sub>7</sub>	−0.011	0.016	−0.004

<sup>a</sup> Values quoted are displacements of ions away from the bulk terminated positions in Å. Displacements constrained by symmetry to be zero are indicated by —. The subscripts on the atom types refer to the layer number of the atom.

the slab is that the wave function should decay to zero at infinity with no constraints on the electrostatic potential perpendicular to the slab. If the bulk stoichiometry is maintained these surfaces are polar and thus unstable due to the generation of a macroscopic electric field. In all cases here the surfaces are modeled by using symmetric, nonstoichiometric slabs which are inherently nonpolar. Calculations were performed for slabs with increasing numbers of layers, and the optimum geometry of the slab for each thickness was found by energy minimization with respect to the atomic positions. The surface energy was found to be converged with respect to slab thickness to better than 0.01 J/m<sup>2</sup> while the Mulliken charges of the central two layers varied from the bulk charge density by less than 0.02|e|. We therefore treat the slab containing seven Al<sup>3+</sup> ions per unit cell as converged with respect to slab thickness.

The initial surface calculation performed was of the Al terminated (0001) surface denoted S<sub>Al</sub>. For the Al<sub>2</sub>O<sub>3</sub> system this termination is known to be the most stable under vacuum conditions.<sup>14</sup> The optimized structure is shown in Table 2 where displacements of the ions away from their bulk terminated positions are given. As expected from the Al<sub>2</sub>O<sub>3</sub> system, the principal displacement is a large downward movement of the surface Al<sup>3+</sup> ion. This is accompanied by a rotation and relaxation of the underlying triangles of fluorine ions.

The second slab considered was the surface terminated by three F<sup>−</sup> ions denoted S<sub>3F</sub>. The geometry of this system has also been fully optimized and the structural parameters are given in Table 3 as displacements from the bulk terminated positions. Again, the principal relaxation is a displacement of the outermost ion of the slab, in this case the F<sup>−</sup> ions. These ions move toward each other and over the second layer Al<sup>3+</sup> ion masking the metal from the external environment.

Two further terminations were produced by successive removal of F ions from the S<sub>3F</sub> slab. These slabs can be denoted as S<sub>2F</sub> and S<sub>1F</sub>. The structure of these slabs is given in Tables 4 and 5. In the S<sub>2F</sub> slab the fluorine ions again move together and over the Al<sup>3+</sup> ion to form zigzag chains running across the surface as shown in Figure 2. For the S<sub>F</sub> system this motion is

**TABLE 4: The Structure of the S<sub>2F</sub> Slab<sup>a</sup>**

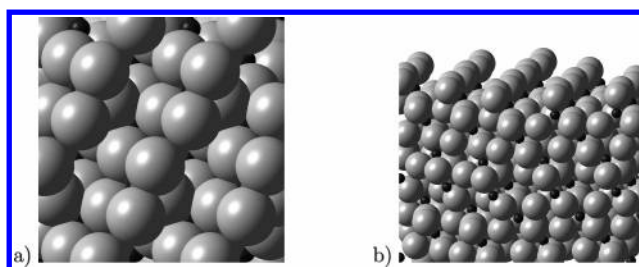
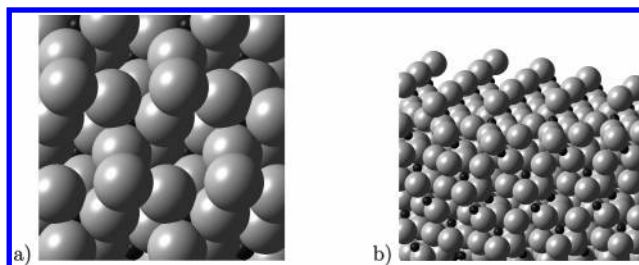
atom	$\Delta x$	$\Delta y$	$\Delta z$
F <sub>1a</sub>	−0.128	−0.055	0.062
F <sub>1b</sub>	−0.238	0.147	0.058
Al <sub>2</sub>	0.138	−0.021	−0.048
F <sub>3c</sub>	−0.021	0.103	0.012
F <sub>3d</sub>	0.005	0.013	0.041
F <sub>3e</sub>	0.037	0.005	−0.085
Al <sub>4</sub>	0.040	−0.017	−0.002
F <sub>5f</sub>	0.045	−0.062	0.007
F <sub>5g</sub>	−0.009	−0.041	−0.047
F <sub>5h</sub>	0.053	−0.003	0.037
Al <sub>6</sub>	0.020	−0.012	−0.003
F <sub>7i</sub>	−0.010	0.046	−0.014
F <sub>7j</sub>	0.056	0.004	0.016
F <sub>7k</sub>	−0.004	−0.024	−0.011

<sup>a</sup> Values quoted are displacements of ions away from the bulk terminated positions in Å. The numerical subscripts on the atom types refer to the layer number of the atom. For the fluorines, the letter subscripts are indicated in Figure 2.

**TABLE 5: The Structure of the S<sub>F</sub> Slab<sup>a</sup>**

atom	$\Delta x$	$\Delta y$	$\Delta z$
F <sub>1a</sub>	0.932	−0.289	0.352
Al <sub>2</sub>	−0.129	−0.015	−0.204
F <sub>3b</sub>	−0.030	−0.226	0.063
F <sub>3c</sub>	−0.214	0.000	−0.023
F <sub>3d</sub>	0.063	0.041	0.234
Al <sub>4</sub>	−0.071	0.005	−0.029
F <sub>5e</sub>	−0.121	0.122	0.013
F <sub>5f</sub>	−0.035	0.076	0.102
F <sub>5g</sub>	−0.112	0.014	−0.072
Al <sub>6</sub>	−0.033	0.011	−0.007
F <sub>7h</sub>	0.019	−0.038	−0.011
F <sub>7i</sub>	0.017	−0.033	−0.063
F <sub>7j</sub>	0.012	−0.034	0.068

<sup>a</sup> Values quoted are displacements of ions away from the bulk terminated positions in Å. The numerical subscripts on the atom types refer to the layer number of the atom. For the fluorines, the letter subscripts are indicated in Figure 3.

**Figure 2.** The optimized S<sub>2F</sub> slab: (a) plane view and (b) side view.**Figure 3.** The optimized S<sub>1F</sub> slab: (a) plane view and (b) side view.

even more extreme with the optimal position for the surface F<sup>−</sup> ion being virtually atop the second layer Al<sup>3+</sup> ion as shown in Figure 3.

An immediate consequence of these relaxations is that for each of the F<sup>−</sup> terminated surfaces considered here the surface



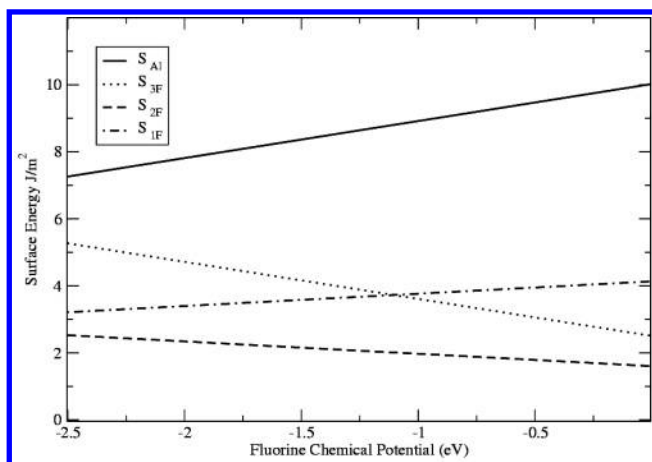


**Figure 4.** Free energies of the four differently terminated slabs as a function of external fluorine partial pressure.

does not expose an  $\text{Al}^{3+}$  ion, which is thus only exposed on the  $\text{S}_{\text{Al}}$  surface where its presence at the surfaces is unavoidable. This is of fundamental importance since it is the  $\text{Al}^{3+}$  ion that would be expected to form the surface Lewis acid center essential to the surface catalysis. Lewis acidity is difficult to quantify in a first principles calculation. However, to partially characterize possible acid sites we have considered the electrostatic potential on a plane 1 Å above the surface. The strong positive potential at the  $\text{S}_{\text{Al}}$  surface and weak negative potentials above the F-terminated surfaces are consistent with the expectation that only the Al terminated surface would be catalytically active.

Having fully optimized the geometry of these slabs, their free energies as a function of external partial pressure of fluorine can be compared. The resultant data are shown in Figure 4. As can be seen, the  $\text{S}_{2\text{F}}$  surface is stable at all realistic F chemical potentials and consequently, under reaction conditions, we would expect this surface to be terminated by a layer containing two  $\text{F}^-$  ions. The potentially chemically active  $\text{S}_{\text{Al}}$  slab is the least stable of the four terminations examined here and consequently is unlikely to be observed in real systems under any reaction conditions.

#### 4. Conclusions

The basal plane of the  $\alpha\text{-AlF}_3$  surface has been studied by using total energy calculations based on hybrid exchange density functional theory. A variety of surface terminations have been considered and their relative stability as a function of external fluorine chemical potential has been evaluated. It has been shown that under all reasonable reaction conditions, the surface would be terminated by a layer containing two  $\text{F}^-$  ions which form a zigzag chain across the surface and mask the  $\text{Al}^{3+}$  ions

from the surrounding environment. This observation is fully consistent with the experimental observation that the perfect  $\alpha\text{-AlF}_3$  surfaces are chemically inert and do not act as a Lewis acid catalyst.

**Acknowledgment.** This work was supported in part by the EU via the 6th Framework Programme (FUNFLUOS, Contract No. NMP3-CT-2004-5005575). The calculations were performed on CCLRC's SCARF system. We would like to thank Prof. Dr. Erhard Kemnitz of the Humboldt University for his help with the preparation of this manuscript.

#### References and Notes

- (1) Kemnitz, E.; Menz, D.-H. *Prog. Solid State Chem.* **1998**, *26*, 97.
- (2) Manzer, L. E.; Rao, V. N. M. *Adv. Catal.* **1993**, *39*, 329.
- (3) Kemnitz, E.; Groß, U.; Rüdiger, St.; Chandra Shekar, S. *Angew. Chem.* **2003**, *115*, 4383.
- (4) Christie, K. O.; Dixon, D. A.; McLemore, D.; Wilson, W. W.; Sheehy, J. A.; Boatz, J. A. *J. Fluorine Chem.* **2000**, *101*, 151.
- (5) Kemnitz, E.; Bozorg Zadeh, H.; Nickkho-Amiry, M.; Winfield, J. M.; Skapin, T. *Zbornik Referatov s Posvetovanja Slovenski Kemijski Dnevi*; Maribor: Slovenia, Sept 20–21, 2001; (Part 2), p 857.
- (6) Bozorgzadeh, H.; Kemnitz, E.; Nickkho-Amiry, M.; Skapin, T.; Winfield, J. M. *J. Fluorine Chem.* **2001**, *107*, 45.
- (7) Dixon, K. W.; Ghorab, M. F.; Winfield, J. M. *J. Fluorine Chem.* **1987**, *37*, 357.
- (8) Murwani, I. K.; Kemnitz, E.; Skapin, T.; Nickkho-Amiry, M.; Winfield, J. M. *Catal. Today* **2004**, *88*, 153.
- (9) Berndt, H.; Bozorg Zadeh, H.; Kemnitz, E.; Nickkho-Amiry, M.; Pohl, M.; Skapin, T.; Winfield, J. M. *J. Mater. Chem.* **2002**, *12*, 3499.
- (10) Barclay, C. H.; Bozorgzadeh, H.; Kemnitz, E.; Nickkho-Amiry, M.; Ross, D. E. M.; Skapin, T.; Thomson, J.; Webb, G.; Winfield, J. M. *J. Chem. Soc., Dalton Trans.* **2002**, *1*, 40.
- (11) Kemnitz, E.; Kohne, A.; Grohmann, I.; Lippitz, A.; Unger, A. W. *S. J. Catal.* **1996**, *159*, 270.
- (12) Krespan, C. G.; Petrov, V. A. *Chem. Rev.* **1996**, *96*, 3269.
- (13) Heß, A.; Kemnitz, E. *J. Catal.* **1994**, *149*, 449/457.
- (14) E.g.: Gomes, J. R. B.; Moreira, I. D. R.; Reinhardt, P.; Wander, A.; Searle, B. G.; Harrison, N. M.; Illas, F. *Chem. Phys. Letts.* **2001**, *341*, 412 and references therein.
- (15) Batyrev, I.; Alavi, A.; Finnis, M. W. *Faraday Discuss.* **1999**, *114*, 33.
- (16) Wang, X. G.; Weiss, W.; Shaikhutdinov, Sh. K.; Ritter, M.; Peterson, M.; Wagner, F.; Schlögl, R.; Scheffler, M. *Phys. Rev. Lett.* **1998**, *81*, 1038.
- (17) Reuter, K.; Scheffler, M. *Phys. Rev.* **2002**, *B65*, art. no. 035406.
- (18) Cahn, J. W. In *Interfacial Segregation*; Johnson, W. C., Blakely, J. M., Eds.; American Society for Metals: Metals Park, OH, 1977; p 3.
- (19) Chase, M. W.; Davies, C. A.; Downey, J. R.; Frurip, D. J.; McDonald, R. A.; Syverud, A. N. *J. Phys. Chem. Ref. Data* **1985**, *14*.
- (20) Saunders, V. R.; Dovesi, R.; Roetti, C.; Orlando, R.; Zicovich-Wilson, C. M.; Harrison, N. M.; Doll, K.; Civalleri, B.; Bush, I. J.; D'Arco, Ph.; Llunell, M. *CRYSTAL 2003 Users's Manual*; University of Torino: Torino, 2004.
- (21) Muscat, J.; Wander, A.; Harrison, N. M. *Chem. Phys. Lett.* **2001**, *342*, 39.
- (22) Spellucci, P. University of Darmstadt. Available from <http://plato.la.asu.edu/donlp2.html>.
- (23) Hoppe, R.; Kissel, D. *J. Fluorine Chem.* **1984**, *24*, 327.
- (24) Pisani, C.; Dovesi, R.; Roetti, C. *Hartree-Fock ab initio Treatment of Crystalline Systems*; Lecture Notes in Chemistry, Vol. 48; Springer-Verlag: Heidelberg, Germany, 1988.